Nickel Ions Biosorption onto Sawmill Wood Waste Products: Kinetics, Equilibrium, and Thermodynamic Investigations

Elizabeth Ogunbamowo Oyebola,[a,b,*] Mohamed Hefnawy,[c] Edwin Andrew Ofudje,[a] Ali El Gamal,[d] James Asamu Akande,[e] and Talha Bin Emran [f,g]

Sawmill wood waste products were used for the biosorption of nickel ions (Ni(II)) from aqueous solution in batch experiments. Effects of physical parameters such as contact time, initial metal concentration, biosorbent dosage, temperature, and pH on the biosorption capacities of both acid-activated sawmill wood waste products (ASWWP) and unactivated sawmill wood waste products (USWWP) were investigated. FT-IR analysis confirmed that hydroxyl, carbonyl, and ether groups are primary contributors to Ni adsorption, through coordination bonding and electrostatic interaction mechanisms. The surface morphology *via* the SEM images showed a rough, irregular surface structure with porous networks prior to adsorption, but some of the pores were blocked after adsorption. Maximum adsorption capacities of 62.3 and 76.3 mg/g were achieved at 120 and 100 min for USWWP and ASWWP at a pH of 5.0 and initial Ni concentration of 180 mg/L, respectively. The pseudo-first-order kinetic model fit well for the USWWP, whereas the pseudo-second-order kinetic model was well-suited for describing the adsorption of Ni(II) ions on ASWWP. The values of enthalpy changes (Δ*H*) for USWWP and ASWWP were 10.2 and 23.4 kJ/mol, respectively, which indicated an endothermic process.

DOI: 10.15376/biores.20.2.3024-3046

Keywords: Biosorption; Kinetics; Nickel; Pollution; Sawmill wood waste

Contact information: a: Department of Chemical Sciences, Mountain Top University, Ogun State, Nigeria; b: Department of Medical Biochemistry, Lagos State University College of Medicine, Ikeja, Lagos, Nigeria; c: Department of Pharmaceutical Chemistry, College of Pharmacy, King Saud University, Riyadh 11451, Saudi Arabia; d: Department of Pharmacognosy, College of Pharmacy, King Saud University, Riyadh 11451, Saudi Arabia; e: Department of Chemistry and Biochemistry, Caleb University, Imota, Lagos State, Nigeria; f: Department of Pathology and Laboratory Medicine, Warren Alpert Medical School, Brown University, Providence, RI 02912, USA; g: Department of Pharmacy, Faculty of Health and Life Science, Daffodil International University, Dhaka 1207, Bangladesh;
** Corresponding author: oyebolaogunbamowo818@gmail.com*

INTRODUCTION

The environment is heavily contaminated by a variety of pollutants, many of which are introduced through human activities. Environmental pollution occurs when the ecosystem becomes overwhelmed and unable to process or neutralize harmful by-products of human actions, such as toxic gases, oil spills, industrial effluent, and household waste (Ofudje *et al*. 2017; Adeogun *et al.* 2018). One major pollutant is nickel, which is frequently released into the environment through various industrial operations. Nickel (Ni) is a naturally occurring element found in the Earth's crust, but human activities have

significantly contributed to its release into the environment. The main sources of nickel pollution include industries such as steel production, electroplating, battery manufacturing, and the production of alloys (Sahoo and Das 2011; Nirav *et al*. 2016; Jain *et al*. 2021; Mohamed *et al.* 2023). Nickel mining and smelting operations also release significant amounts of nickel-containing dust and wastewater, leading to contamination of nearby ecosystems (Sahoo and Das 2011; Jain *et al*. 2021; Mohamed *et al.* 2023). Other sources of nickel in the environment are burning of coal, oil, incineration of waste materials containing nickel, (such as metal products, batteries, and electronic waste), agricultural practices (such as fertilizers and pesticides applications), and natural sources (including volcanic eruptions, forest fires, and the weathering of nickel-containing rocks). These can naturally release nickel into the environment (Sahoo and Das 2011; Edwin *et al*. 2021; Jain *et al*. 2021; Mohamed *et al.* 2023).

To protect human health and the environment, regulatory agencies such as the World Health Organization (WHO) and the United States Environmental Protection Agency (USEPA) have established guidelines for the maximum allowable concentrations of nickel in drinking water. For instance, the USEPA has set the maximum contaminant level (MCL) for nickel in drinking water at 0.1 mg/L (100 µg/L) (Edwin *et al.* 2021; Jain *et al*. 2021). Nickel pollution in the environment poses several risks to human health, wildlife, and ecosystems. Nickel is toxic when ingested or inhaled in excessive amounts, and chronic exposure can lead to respiratory problems, skin rashes (nickel dermatitis), and allergic reactions (Buxton *et al.* 2019; Edwin *et al*. 2021; Jain *et al*. 2021). Prolonged exposure to nickel dust or fumes can increase the risk of lung and nasal cancers as well cause kidney and liver damage when exposed at high levels of nickel intake (Buxton *et al.* 2019; Jain *et al*. 2021; Wasefa *et al*. 2022). Long term exposure to nickel has also been reported to contribute to cardiovascular diseases, such as heart disease and hypertension (Jain *et al*. 2021; Wasefa *et al*. 2022). The need to therefore eliminate nickel ions from water bodies becomes imperative.

Several methods, such as electro-dialysis, advanced oxidation processes, coagulation/flocculation, precipitation, ion-exchange, among others have been employed to remove Ni(II) ions from wastewater (Edwin *et al.* 2021; Shrestha *et al*. 2021; Ofudje *et al*. 2023). However, these methods are often expensive, inefficient, and generate large amounts of sludge (Ofudje *et al*. 2023). Biosorption, which utilizes materials such as bacteria, fungi, yeast, and agricultural waste as biosorbents, has proven to be an effective and economical solution for removing metal ions, including nickel ions, from contaminated water (Adeogun *et al*. 2012; Ofudje *et al.* 2014). Biosorption refers to the removal of metal ions through passive adsorption or complexation by biological materials. Biosorbents are cost-effective, widely available, and efficient, offering significant potential for regeneration and reusability. Various biosorbents have been used for this purpose, including lime peel (Sudha *et al*. 2015), *Chrysanthemum indicum* flowers biochar (Vilvanathan and Shanthakumar 2016), date seed (Mahdi *et al*. 2018), corn cobs (Shi *et al*. 2018), local rice bran (Zafar *et al*. 2015), corn stalk (Li *et al*. 2018), fish scale derived nano-rod hydroxyapatite (Edwin *et al.* 2021), Sugarcane bagasse (Blessing *et al*. 2021), copper oxide nanoparticles (Jain *et al*. 2021) and *Pinus sylvestris* sawdust (Chanda *et al*. 2021).

Wood sawmills in Nigeria are major contributors to the country's economy due to the high demand for timber and wood products. However, they also generate significant amounts of waste during wood processing. Part of the waste generated from sawmills often consists of fine wood particles produced during sawing operations, which is known as

sawdust. Sawdust has been used as an adsorbent for the removal of contaminants from wastewater. For instance, the sorption of some selected toxic metal ions on pine sawdust *in situ* immobilized by polyaniline was investigated by Yanovska *et al.* (2022), and the results demonstrated that pine sawdust, when immobilized with polyaniline, adsorbed up to 56 mg/g of Fe(III) ions from slightly alkaline solutions (pH 8) within a short period. Kovacova *et al.* (2020) investigated the influence of wooden sawdust on the treatments on the adsorption of Cu(II) and Zn(II); the study found that the initial concentrations of heavy metals greatly affected the adsorption capacity of sawdust achieving a highest adsorption efficiency 94.3% for copper at pH 6.8 and 98.2% for zinc at pH 7.3 respectively. Across all sawdust types, modified sorbents exhibited superior sorption efficiency compared to untreated sawdust and that the initial pH showed a greater increase with modified sawdust, reaching 8.2 for zinc removal using NaOH-treated spruce, before gradually decreasing to 7.0 for Zn(II) with the same sorbent.

The kinetics, mechanism, and equilibrium of the adsorption of heavy metal ions by beech sawdust was documented by Dragana *et al.* (2013), who showed that the maximum adsorption capacity was achieved at pH levels above 4, with capacities of 4 to 4.5 mg/g for Cu^{2+} and Ni^{2+} ions, and 2 mg/g for Zn^{2+} ions, indicating selectivity towards copper and nickel ions over zinc. The adsorption kinetics followed a pseudo-second-order reaction model, while the equilibrium data exhibited a strong fit to the Langmuir equation. It follows that the adsorption process primarily occurs through an ion exchange mechanism, where heavy metal ions replace calcium within the sawdust cell structure. The research work of Liu *et al.* (2020) compared the adsorption capacities of activated carbon, peanut shell, and sawdust, and it was observed that the adsorption increased with time before reaching equilibrium, while higher initial metal concentrations led to greater adsorption but lower removal efficiency. Activated carbon exhibited the highest adsorption capacity, followed by peanut shell, with sawdust showing the lowest efficiency. The process followed the Langmuir isotherm and pseudo-second-order kinetic models. The adsorption efficiencies of heavy metal ions followed the order: lead > copper > cadmium.

The amount of waste produced varies depending on the size of the sawmill, type of machinery used, and the type of wood processed. The large volume of waste generated by sawmills in Nigeria has serious environmental consequences, affecting air, water, soil, and overall ecological balance. In many areas, sawmill waste, especially sawdust, is burned openly to clear space, releasing large amounts of carbon dioxide (CO_2), particulate matter, and other harmful gases into the atmosphere. Accumulated wood waste, particularly in wet environments, can become breeding grounds for mosquitoes and other disease-carrying insects, thereby increasing the risk of malaria and other vector-borne diseases in nearby communities. Since the same materials contain functional groups such as hydroxyl, carbonyl, amine groups, and many others, their conversions as sorption sites for metal ions in solution will be of great benefits not only to eliminate pollutants but also serves a means of adding values to agricultural waste. This research therefore introduces sawmill wood waste as a low-cost, sustainable, and widely available biosorbent, addressing both environmental pollution and waste management. Green technology is promoted by repurposing industrial waste for wastewater treatment, reducing dependency on synthetic adsorbents. Unlike many studies that focus solely on adsorption capacity, this study provides an in-depth analysis of the kinetics, equilibrium, and thermodynamics, offering a complete understanding of the adsorption mechanism. The aim of this study is to investigate the biosorption of nickel (Ni^{2+}) ions onto sawmill wood waste products by analyzing the kinetics, equilibrium, and thermodynamic aspects of the process. This

research identified the functional groups responsible for metal ion binding and the changes that took place on the surface of the adsorbent using techniques such as Fourier transform infrared (FTIR) spectrometry, and scanning electron microscopy (SEM). The evaluation of different kinetic models (*e.g.*, pseudo-first-order, and pseudo-second-order models) to determine the best-fitting adsorption mechanism was also done. Finally, the assessment of the adsorption capacity and interaction between nickel ions and the biosorbent through fitting of experimental data to isotherm models to describe the adsorption behavior was done.

MATERIALS AND METHODS

Preparation of Adsorbent and Adsorbate

Wood waste from a local sawmill in Ifo, Ogun State, Nigeria, was collected and processed. The waste was thoroughly washed with distilled water, filtered, and sun-dried for five days. The dried biomass was then ground into a fine powder using a mechanical grinder and sieved through a 250-mesh sieve. Approximately 50 g of the finely ground biosorbent was immersed in 250 mL of 0.1M HNO_3 solution in a 500 mL conical flask for 12 h. Afterward, it was filtered and dried at 100 °C for 3 h. The dried, acid-treated biomass was termed acid-activated sawmill wood waste products (ASWWP), while the untreated portion was referred to as unactivated sawmill wood waste products (USWWP). All chemicals used in this study were of analytical grade and procured from Sigma Aldrich (India), and they were utilized as received. A 1000 mg/L stock solution of Ni(II) was prepared by dissolving nickel nitrate hexahydrate [$Ni(NO_3)_2 6H_2O$] in deionized water. Working solutions were subsequently obtained by diluting this stock solution. The pH of the solutions was adjusted using 0.1 M HCl or 0.1 M NaOH, measured with a digital pH meter.

Biosorption Batch Experiments

Various concentrations of nickel were prepared, with 30 mg of the biosorbent placed in 250 mL Erlenmeyer flasks containing 25 mL of solution. The biosorption experiments were conducted using a rotary thermostat shaker (BIOBASE Thermo Shaker Incubator, Model: BK-TSI10) at a speed of 200 rpm. After an equilibrium contact time of 120 min, the mixture was filtered using filter paper, and the filtrate was analyzed for nickel content using an atomic absorption spectrophotometer (UNICAM model 929, Thermo Fisher Scientific, Waltham, Massachusetts, USA). The effects of parameters such as initial metal concentration, sorbent dosage, temperature, and pH were also investigated. All experiments were performed in triplicate, and the mean values were reported. The amount adsorbed, denoted as q_e, and the percentage adsorbed were calculated using Eq. 1 and Eq. 2 respectively,

$$\text{Amount adsorbed, } q_e = \frac{C_o - C_e}{m} V \quad (1)$$

$$\text{Percentage adsorbed } q_e = \frac{C_o - C_e}{C_o} x100 \quad (2)$$

where C_o and C_e are the initial and equilibrium concentrations of adsorbate in mg/L, m is the mass of the biomass used in g, and V is the volume of the adsorbate in L.

Desorption Studies

To assess the viability of the biosorption process, sorption-desorption studies were conducted on the already used biosorbent. After reaching equilibrium, the metal ions were carefully decanted, and desorption was carried out using 0.1 M acetic acid. In these experiments, 35 mg of the exhausted biosorbent was equilibrated with 25 mL of Ni(II) ion solution for 120 min at a speed of 150 rpm. The mixture was then filtered, and the filtrate was analyzed for nickel ion content using atomic absorption spectroscopy (AAS). This procedure was repeated for four cycles, following the same experimental protocol and the percentage desorption (%D) was estimated using Eq. 3,

$$\%D = \frac{AD}{AA} X100 \quad (3)$$

where D is the desorption, AD is the amount (g) desorbed, and AA is the amount (g) adsorbed. All experiments were performed in triplicate, and the mean values were reported.

RESULTS AND DISCUSSION

Effect of Ni(II) Ion Concentration and Contact Time on Adsorption Capacity

The comparative analysis of the effect of initial nickel ions concentration and time of contact on the adsorption of Ni(II) ions by USWWP and ASWWP revealed important distinctions in adsorption performance under varying conditions.

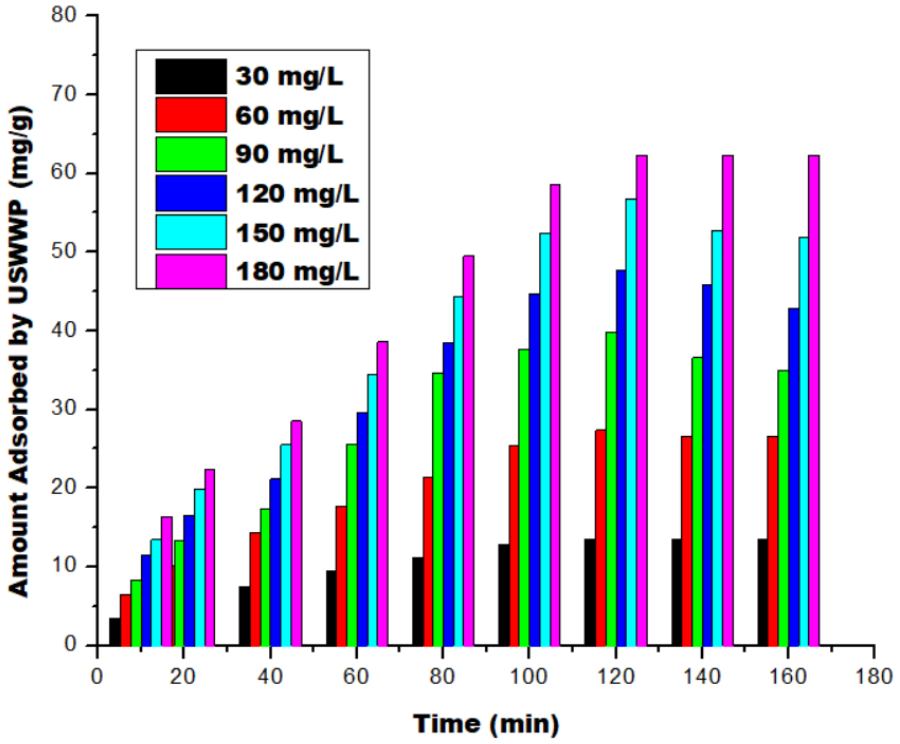

Fig. 1. Amount of Ni(II) adsorbed by unactivated sawmill wood waste

The adsorption capacity of the USWWP rose significantly from 16.4 mg/g to 62.3 mg/g as time increased from 10 to 120 min at initial nickel ions concentration of 180 mg/L (Fig. 1). After 120 min, there was no further increase in adsorption capacity, indicating that

equilibrium was reached around this time. This high adsorption at a high initial concentration suggests that the adsorption sites were initially unsaturated and readily available for Ni ions until reaching saturation at 120 min. However, at a lower concentration of 30 mg/L, the adsorption capacity increased from 3.5 to 13.6 mg/g as time increased from 10 to 120 min, and no further increase in adsorption capacity occurred beyond 120 min. The lower increase in adsorption capacity at 30 mg/L compared to 180 mg/L suggests that fewer Ni ions were available to occupy adsorption sites, resulting in a lower overall capacity.

In the case of the ASWWP, at a concentration of 180 mg/L, the adsorption capacity increased from 23.2 to 76.3 mg/g within the first 100 min, reaching a peak more quickly than the USWWP. It was observed that after 100 min, the adsorption capacity slightly decreased to 72.3 mg/g at 160 min, which could indicate some desorption of Ni ions from the adsorbent surface (Fig. 2).

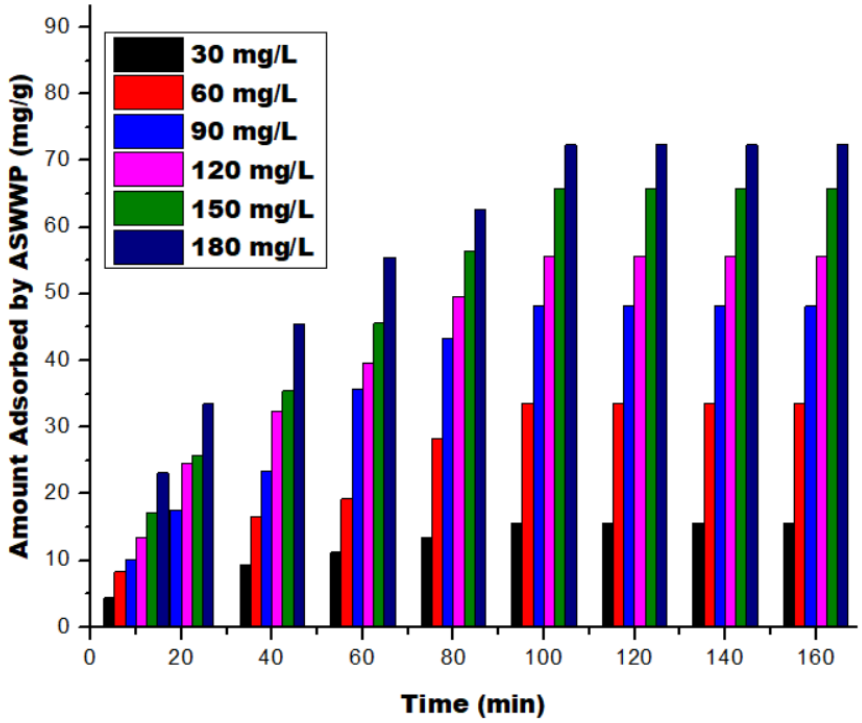

Fig. 2. Amount of Ni(II) adsorbed by acid-treated sawmill wood waste

The faster and higher capacity increase at high initial concentrations indicates improved adsorption properties due to acid activation, which enhances surface area or functional group availability. At low concentration of 30 mg/L, however, the adsorption capacity rose from 4.6 to 15.6 mg/g as time increased from 10 to 100 min, with no further increase up to 160 min. This trend was similar to that of USWWP at lower concentrations, but the slightly higher adsorption capacity (15.6 mg/g compared to 13.6 mg/g) also reflects the enhanced properties of acid-activated wood waste.

Generally, the adsorption capacity was smaller for USWWP compared to the acid-activated wood waste, particularly at the higher initial concentration, as equilibrium was achieved only after 120 min, whereas for the acid-treated sample, equilibrium was attained faster after just 100 min. The earlier surge in adsorption with respect to time can be attributed to the vacant sites on the adsorbent surface, which effectively adsorbed the metal

ions (Adeogun *et al*. 2012; Edwin *et al*. 2021). But as the reaction proceeded, these sites became filled up, leading to saturation on the adsorbent surface. This could explain why adsorption was not noticeable at a time higher than 120 and 100 min for USWWP and ASWWP (Adeogun *et al*. 2012; Edwin *et al*. 2021). The ASWWP achieved higher adsorption amounts more quickly, reaching peak adsorption capacity at around 100 min, which was 20 min earlier than the raw adsorbent indicating a more efficient adsorption process likely due to enhanced surface characteristics provided by acid treatment.

Effect of pH on Percentage Removal

The effect of pH on the adsorption of Ni(II) ions by USWWP and ASWWP highlights how solution pH influenced adsorption capacity. Changes in surface charge and ionization of active sites on the adsorbents are shown in Fig. 3.

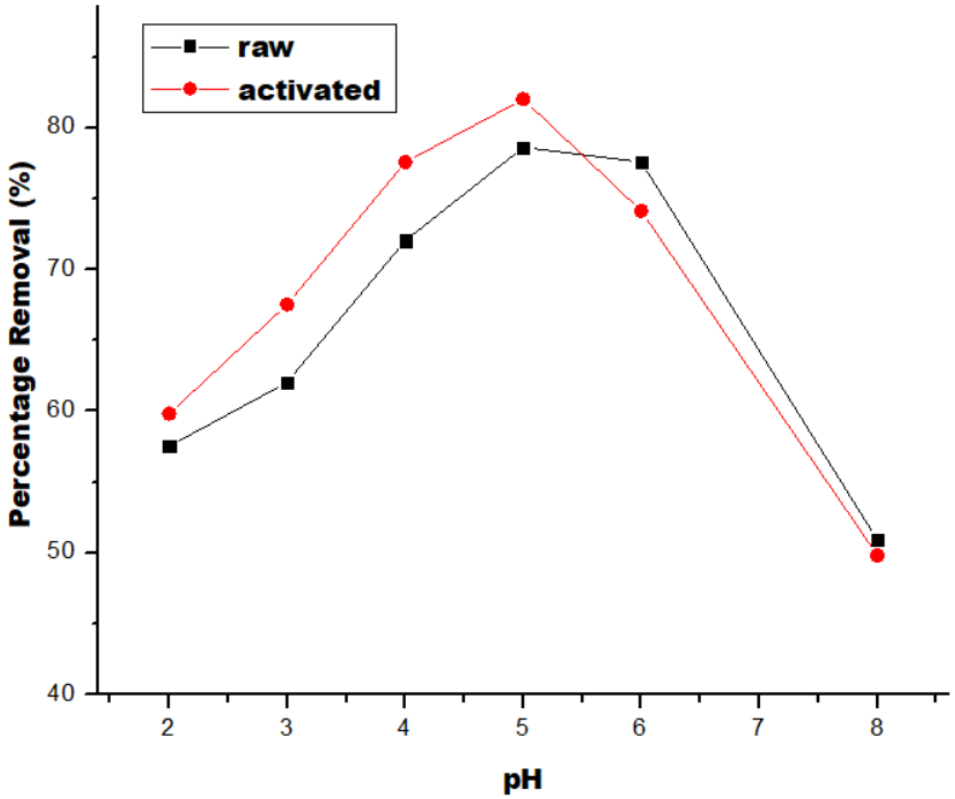

Fig. 3. Percentage removal of Ni(II) ions against pH by raw and acid-treated sawmill wood waste

With the USWWP, the percentage removal of Ni(II) ions increased from 57.4% at pH 2.0 to 78.6% at pH 5.0, whereas, that of the activated adsorbent increased from 59.8% at pH 2.0 to a peak of 82.0% at pH 5.0, slightly higher than the USWWP. At low pH (pH 2), both materials demonstrated lower adsorption capacity (57.4% for USWWP and 59.8% for ASWWP), likely due to protonation of surface functional groups, which reduces available binding sites for Ni ions (Ofudje *et al*. 2017; Adeogun *et al*. 2018; Blessing, *et al*. 2021). This increase suggests that as the pH rises from 2 to 5, more active sites on the raw adsorbent surface become available, such that the surfaces become more favorably charged for Ni ion binding. At low pH (acidic conditions), the surface of the adsorbent may be positively charged, leading to electrostatic repulsion with Ni(II) ions, which are also positively charged, but with increasing pH, this repulsion decreases or becomes an

attraction, allowing more Ni ions to be adsorbed (Ofudje *et al*. 2017; Adeogun *et al*. 2018). At a higher pH 8.0, the percentage removal decreased sharply to 50.9% and 49.8% for USWWP and activated adsorbent, respectively, which suggests that a further increase in pH beyond 5 reduces the adsorption efficiency. This decrease may be due to the precipitation of Ni(II) as $Ni(OH)_2$ at higher pH levels. This would cause a change in the adsorbent's surface properties, making it less favorable for Ni ion adsorption (Vilvanathan and Shanthakumar 2016). The observed pH effects should be discussed in light of expected changes in the predominant species of nickel ions present in solution. It was observed further that the ASWWP demonstrated better adsorption efficiency at each pH level than the raw material, which may be due to the presence of additional acidic functional groups introduced by the acid treatment as these groups may enhance ion exchange or provide better binding sites for Ni ions, especially as the pH approaches neutral.

Effect of Adsorbent Dosage on Percentage Removal

The effect of adsorbent dosage on the adsorption of Ni(II) ions by USWWP and ASWWP revealed key differences in the efficiency and saturation levels of each adsorbent, as shown in Fig. 4.

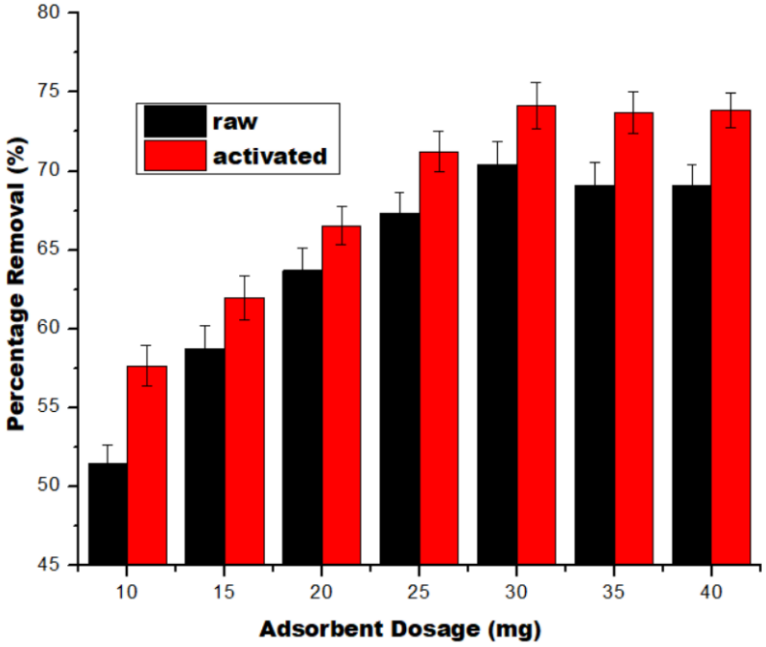

Fig. 4. Percentage removal of Ni(II) ions against adsorbent dosage by raw and acid-treated sawmill wood waste products

For the USWWP, the percentage removal of Ni(II) ions increased from 51.4% at a dosage of 10 mg to 71.0% at 25 mg, while that of the acid-activated adsorbent increased from 57.6% at 10 mg to 74.1% at 30 mg, showing both a higher initial removal rate and a higher maximum percentage removal compared to the unactivated material. This increase indicates that a higher dosage provided more surface area and active sites for adsorption, allowing a larger amount of Ni ions to be removed from the solution. However, after 25 and 30 mg, no further increase in percentage removal was observed, suggesting that the adsorption sites became saturated and additional adsorbent did not significantly improve the removal efficiency (Chukwuemeka-Okorie *et al*. 2018; Blessing, *et al*. 2021). This

plateau may be due to an equilibrium between Ni ions and available adsorption sites on the sawmill wood waste. At every dosage level, the ASWWP achieved higher percentage removal than the USWWP, and this enhanced efficiency is likely due to the improved porosity and increased number of active sites available for adsorption following acid treatment as the acid activation, which likely resulted in the displacement of calcium ions from the adsorbent surface, thus rendering the cites available for other metal ions.

Kinetics Investigations

Pseudo-first order kinetic model

In the context of adsorption kinetics, the pseudo-first-order model (PFOM) can be used to fit data for the adsorption rate of Ni(II) ions onto the sawmill wood waste samples. Comparing the kinetic parameters for USWWP and ASWWP samples provides insights into how well the adsorption process follows the PFOM, as well as differences in adsorption efficiency, rate constants, and model fit. The PFOM can be expressed in Eq. 4 below (Akpomie and Dawodu 2014; Blessing *et al*. 2021):

$$In(q_e - q_t) = Inq_t - k_1 t \quad (4)$$

The amounts of Ni adsorbed at time *t* and at equilibrium, expressed in mg/g, are represented as q_t and q_e, respectively. The rate constant of the PFOKM, is denoted as $k_1(min^{-1})$, was determined as in Fig. 5, with the calculated values provided in Tables 1 and 2, respectively. To validate the appropriateness of the best kinetic model, the data were analyzed using the sum of squares error (%SSE) to evaluate the fit of each model, as described in Eq. E below (Adeogun *et al*. 2012),

$$\%SSE = \sqrt{\frac{(q_{(\exp)} - q_{(cal)})^2}{N}} \quad (5)$$

where *N* indicates the number of data points. A higher coefficient of determination (R^2), value and a lower %SSE indicate a better goodness of fit.

Both the USWWP and ASWWP samples showed a reasonable alignment between $q_{e\{exp\}}$ and $q_{cal\{cal\}}$ with the raw sample demonstrating a closer fit. The acid-treated sample had a wider range in $q_{e\{exp\}}$ values, indicating an increase in adsorption capacity due to acid activation. However, the greater discrepancy between $q_{e\{exp\}}$ and $q_{cal\{cal\}}$ for the ASWWP sample suggests that this model may not fully capture the adsorption dynamics post-treatment, possibly due to the introduction of more active sites or a change in the adsorption mechanism. From the study on the coefficient of determination (R^2), it was observed that both the raw sample (0.996 to 0.998) and treated sample (0.93 to 0.989) had high values (Table 1), indicating the alignment of both samples with PFOM. This was supported based on the information obtained from %SSE where the USWWP sample has a lower value (0.004 to 0.04), indicating that the PFOM accurately describes its adsorption kinetics. The ASWWP sample, with a higher values (0.027 to 0.207), showed a less accurate fit, possibly due to the increased heterogeneity or complexity introduced by acid treatment.

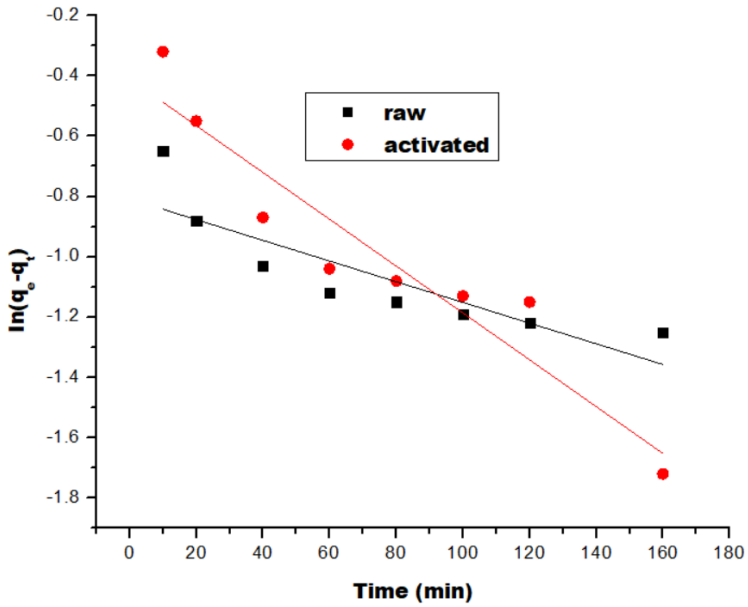

Fig. 5. Pseudo-first-order plots for the adsorption of Ni(II) ions by raw and acid-treated sawmill wood waste products

The acid-treated sample exhibited a much broader range of k_1 values (0.014 to 0.82 min^{-1}) compared to the raw sample (0.016 to 0.078 min^{-1}). This indicates that acid treatment enhanced the adsorption rate at its peak, suggesting faster adsorption kinetics. This improvement may result from increased porosity, higher surface area, or additional functional groups introduced by the acid treatment that make adsorption sites more accessible.

Pseudo-second order kinetic model

The pseudo-second-order kinetic model (PSOKM) is frequently used to describe adsorption processes. A comparative analysis of the PSOKM for USWWP and ASWWP is provided using Eq. 6 (Adeogun *et al*. 2012; Izinyon *et al*. 2016; Blessing *et al*. 2021**)**,

$$\frac{t}{q_t} = \frac{1}{k_2 q_e^2} + \frac{1}{q_e} t \quad (6)$$

where k_2 ($g.mg^{-1}min^{-1}$) denotes the rates constant of second order adsorption which was determined using Fig. 6, with the calculated values provided in Tables 1 and 2, respectively.

Both samples show that $q_{e\{cal\}}$ was reasonably aligned with $q_{e\{exp\}}$, although the raw sample had a wider range of calculated capacities. The USWWP sample demonstrated higher adsorption capacities, indicating improved efficiency and performance after treatment, particularly at higher concentrations. The sample exhibited a broader range and higher maximum rate constant (k_2) with values in the range of 0.138 to 1.667 $g/mg \cdot min^{-1}$ (Table 2) compared to the raw sample values in the range of 0.019 to 0.892 $g/mg.min^{-1}$. This demonstrates that acid treatment enhanced the kinetics of adsorption, leading to a faster uptake of Ni(II) ions. Both samples exhibited high R^2 values, though much higher in the case of the acid treated samples, suggesting that the PSOKM is an effective representation of the adsorption kinetics for ASWWP. This was supported based on the findings from the sum of squares error (%SSE), which revealed that the acid-treated sample

exhibited lower %SSE values (0.003 to 0.038) compared to the raw sample (0.017 to 0.14), indicating that the pseudo-second-order model fit the adsorption kinetics more accurately for the acid-treated material.

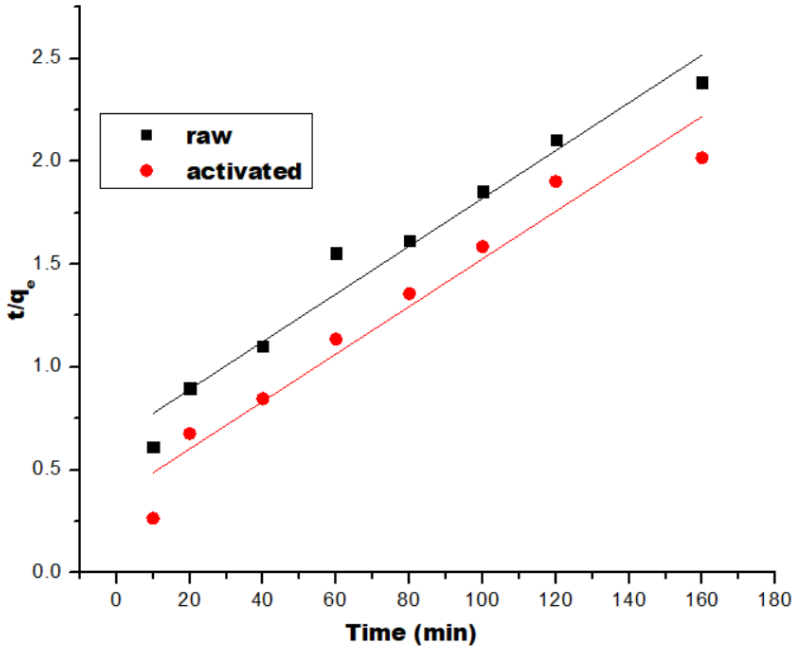

Fig. 6. Pseudo-second-order plots for the adsorption of Ni (II) ions by raw and acid-treated sawmill wood waste

Table 1. Kinetics Constants for the Adsorption of Ni(II) Ions by USWWP

	C_o (mg/L)	30.000	60.000	90.000	120.000	150.000	180.000
First order	Q_e(exp) (mg/g)	13.550	27.340	39.560	48.980	54.501	62.323
	Q_e(cal) (mg/g)	12.352	26.342	39.142	40.216	55.023	64.373
	k_1 (min^{-1})	0.016	0.023	0.025	0.039	0.055	0.078
	R^2	0.998	0.996	0.998	0.996	0.996	0.998
	%SSE	0.040	0.016	0.004	0.008	0.004	0.013
Second order	q_e (cal) (mg/g)	17.756	35.969	48.014	56.182	67.041	75.505
	k_2 (g/mg/min)	0.019	0.268	0.431	0.479	0.679	0.892
	R^2	0.997	0.996	0.989	0.997	0.987	0.995
	%SSE	0.139	0.141	0.040	0.017	0.052	0.082
Intra particle	K_p (mg/g·min$^{0.5}$)	1.127	2.006	4.378	5.019	7.207	10.022
	C_i (mg/g)	0.407	0.535	1.228	3.504	5.103	8.032
	R^2	0.985	0.995	0.988	0.996	0.996	0.996

Table 2. Kinetics Constants for the Adsorption of Ni(II) Ions by ASWWP

	C_o (mg/L)	30.000	60.000	90.000	120.000	150.000	180.000
First order	Q_e(exp) (mg/g)	15.670	33.600	48.800	55.621	62.066	76.34
	Q_e(cal) (mg/g)	22.930	44.805	57.502	69.482	70.352	81.483
	k_1 (mins^{-1})	0.014	0.018	0.024	0.045	0.058	0.082
	R^2	0.967	0.987	0.998	0.938	0.930	0.989
	% SSE	0.207	0.149	0.066	0.094	0.051	0.027
Second order	Q_e(cal) (mg/g)	17.001	32.404	47.712	58.012	63.221	77.015
	k_2 (g/mg/min)	0.138	0.262	0.424	0.805	1.263	1.667
	R^2	0.998	0.996	0.987	0.997	0.998	0.998
	% SSE	0.038	0.016	0.008	0.016	0.007	0.003

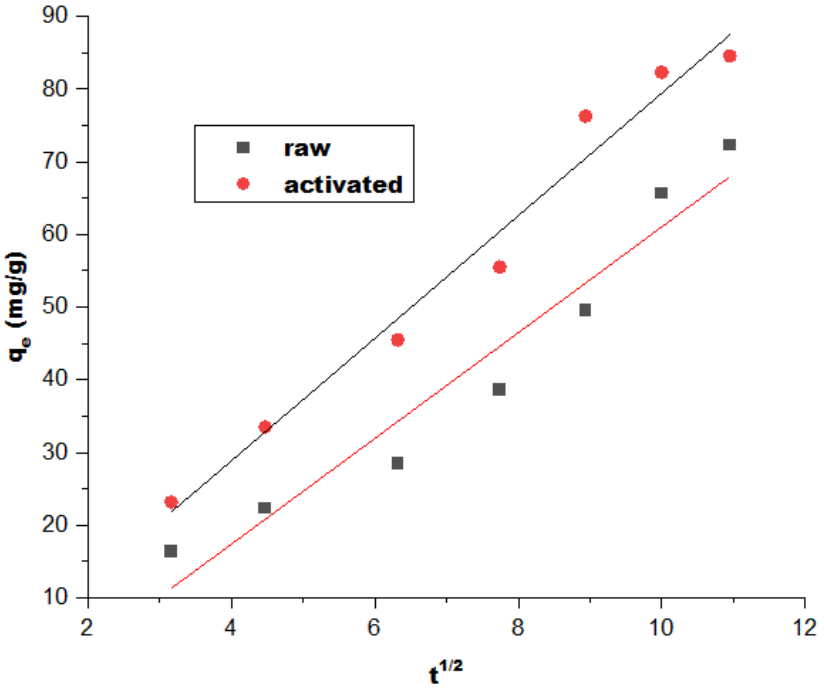

Fig. 7. Intraparticle diffusion model plots for the adsorption of Ni (II) ions by raw and acid-treated sawmill wood waste

Intraparticle diffusion kinetic model

The equation for intraparticle diffusion in adsorption is given by the Weber-Morris model. This model is based on how adsorbate molecules move inside the pores of the adsorbent and can be expressed as given in Eq. 7 (Duran *et al.* 2011; Ofudje *et al.* 2017**)**,

$$q_t = K_p t^{1/2} + C_i \quad (7)$$

where K_P (mg/g·min$^{0.5}$) denotes the intraparticle diffusion rate constant, and C_i represents the boundary layer (mg/g), indicating the external mass transfer effect determined from Fig. 7, with the estimated values given in Tables 1 and 2, respectively. The high R^2 values

from both raw and acid-activated samples (above 0.97) confirm that intraparticle diffusion is a key part of the mechanism. The adsorption mechanism generally follows three multiple stages with the external mass transfer (film diffusion) being the first stage where nickel ions move from the bulk solution to the outer surface of the adsorbent. The second stage is the intraparticle diffusion where nickel ions diffuse into the internal pores of the sawmill wood waste, and the final stage is the surface interaction where the nickel ions interact with active sites on the adsorbent surface (Duran *et al*. 2011; Ofudje *et al*. 2017). The K_p values are consistently higher for acid-treated wood waste (up to 19.8 as against 10.0 for raw wood), and this suggests that acid treatment enhances the pore structure, increasing the diffusion rate of nickel ions. The C_i values were higher in the acid-treated sample, reaching 9.029 compared to 8.032 in the raw sample. This indicates that acid treatment increases external mass transfer resistance, likely due to surface modifications improving adsorption sites.

An excellent fit to the PSOKM model, and as well as to the PFOKM in another case, suggests that the adsorption rate is governed by the diffusion and interaction of adsorbate molecules within a porous network (Hubbe *et al.* 2019). This implies that the rate of the adsorption process is greatly influenced by pore diffusion and surface interactions within the adsorbent structure.

Isotherms Study

Langmuir isotherm

Langmuir isotherm model provides insight into the adsorption characteristics of raw and acid-treated sawmill wood waste, describing the monolayer adsorption capacity and affinity of the adsorbents for Ni(II) ions. The Langmuir isotherm equation is given by Eq. 8 (Hlihor *et al*. 2015; Blessing, *et al*. 2021),

$$\frac{C_e}{q_e} = \frac{1}{Q_m b} + \frac{1}{Q_m} C_e \quad (8)$$

where q_e (mg/g) represents the amount of Ni adsorbed per unit mass of the adsorbent, Q_m(mg/g) denotes the maximum adsorption capacity corresponding to monolayer coverage, and b (L/mg) is the Langmuir constant, indicating the affinity between the adsorbent and adsorbate. The separation factor or dimensionless constant (R_L) is given by Eq. 9 (Adeogun *et al*. 2012; Hlihor *et al*. 2015),

$$R_L = \frac{1}{(1 + bC_i)} \quad (9)$$

where C_i stands for initial Ni concentration (mg/L).

These constants were evaluated from Fig. 8, and their values are listed in Table 3. The acid-treated sample had a higher Q_{max} of 76.3 mg/g when compared with the raw sample value of 68.8 mg/g, suggesting that acid activation enhanced the maximum adsorption capacity. This is likely due to the displacement of calcium ions by protons on the adsorbent surface, thus enabling more sites of adsorption, which allows more Ni ions to be adsorbed. The ASWWP has a lower R_L value (0.058) compared to the raw sample (0.223), indicating that the acid-treated material had a stronger affinity for Ni ions. Since the value of R_L for both adsorbents fell within the zero to one range, it indicates favorable adsorption, with strong affinity between Ni ions and the adsorbent surface (Adeogun *et al*. 2012; Hlihor *et al*. 2015). The USWWP sample had a higher coefficient of determination

(R^2) value of 0.997 compared to the acid-treated sample (0.947), suggesting a better alignment of the raw sample's adsorption data with the Langmuir isotherm and that the adsorption data for the acid-treated wood waste may not align as closely with the Langmuir isotherm model. This implies that the USWWP sample follows a more ideal monolayer adsorption behavior, possibly due to the modified surface properties after acid treatment.

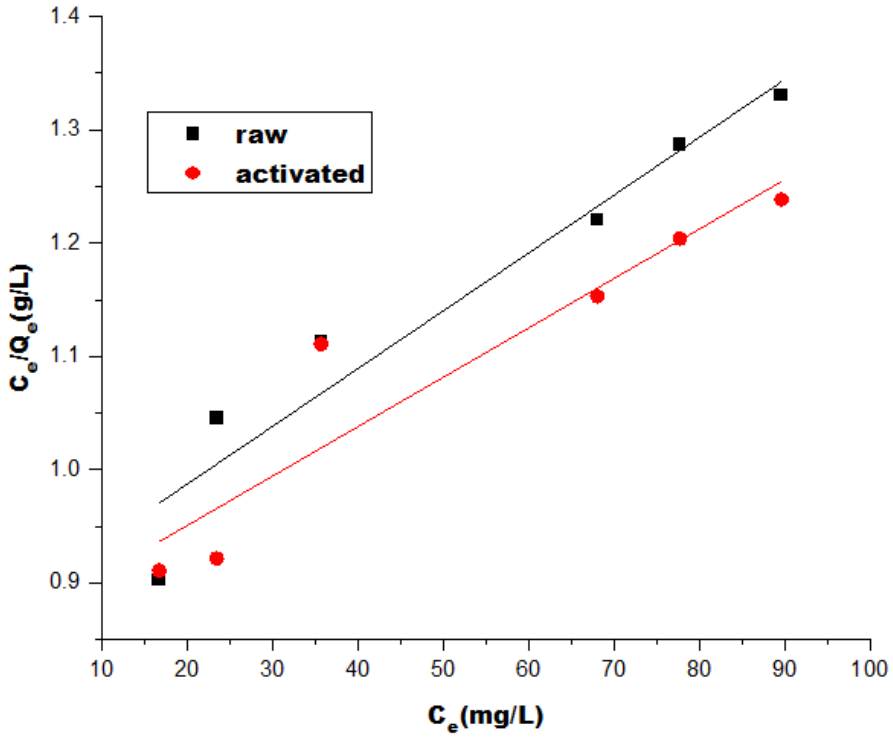

Fig. 8. Langmuir plots for the adsorption of Ni(II) ions by raw and acid-treated sawmill wood waste products

Table 3. Isotherm Parameters for the Adsorption of Ni(II) Ions by Raw and Acid-treated Wood Waste Products

Isotherms	Parameters	Raw	Acid-Treated
Langmuir	q_{max}(mg/g)	68.752	76.342
	R_L (mg/L)	0.223	0.058
	R^2	0.997	0.947
Freundlich	K_F (mg/g)	43.066	79.176
	1/*n*	0.213	0.012
	R^2	0.954	0.988

Freundlich isotherm model

The Freundlich isotherm model is used to describe adsorption on heterogeneous surfaces, providing insights into adsorption intensity and capacity. The parameters of the Freundlich models for the adsorption of Ni(II) ions by USWWP and ASWWP samples were obtained from the Eq. 10 below (Hlihor *et al*. 2015; Blessing, *et al*. 2021),

$$Inq_e = InK_F + \frac{1}{n} InC_e \quad (10)$$

where K_F reflects the adsorption capacity constant of the Freundlich, representing how well Ni(II) ions are adsorbed onto the heterogeneous surface of the material, while the Freundlich intensity parameter ($1/n$) indicates the adsorption intensity and favorability. Those values are obtained from Fig. 9, and the results are listed in Table 3. The ASWWP sample had a much higher K_F value of 79.2 compared to the raw sample (43.1 mg/g), reflecting the enhanced adsorption capacity imparted by acid activation. The acid-treated sample's value of $1/n$ (0.012) was significantly lower than that of the raw sample (0.213), indicating a stronger adsorption intensity and higher affinity for Ni ions. Acid treatment appeared to significantly increase the strength of Ni ion binding, suggesting that the adsorbent surface had become more favorable for adsorption as a result of the acid treatment. Both the USWWP and ASWWP samples exhibited high R^2 values, though the acid-treated sample showed a higher value (0.988) compared to the raw sample (0.958). This suggests that both the Freundlich and Langmuir model were suitable for describing Ni ion adsorption on the adsorbents. The comparison analysis of the adsorption capability of sawmill wood waste with other documented adsorbents in literature is depicted in Table 4, which showed favorable adsorption potency towards nickel ions.

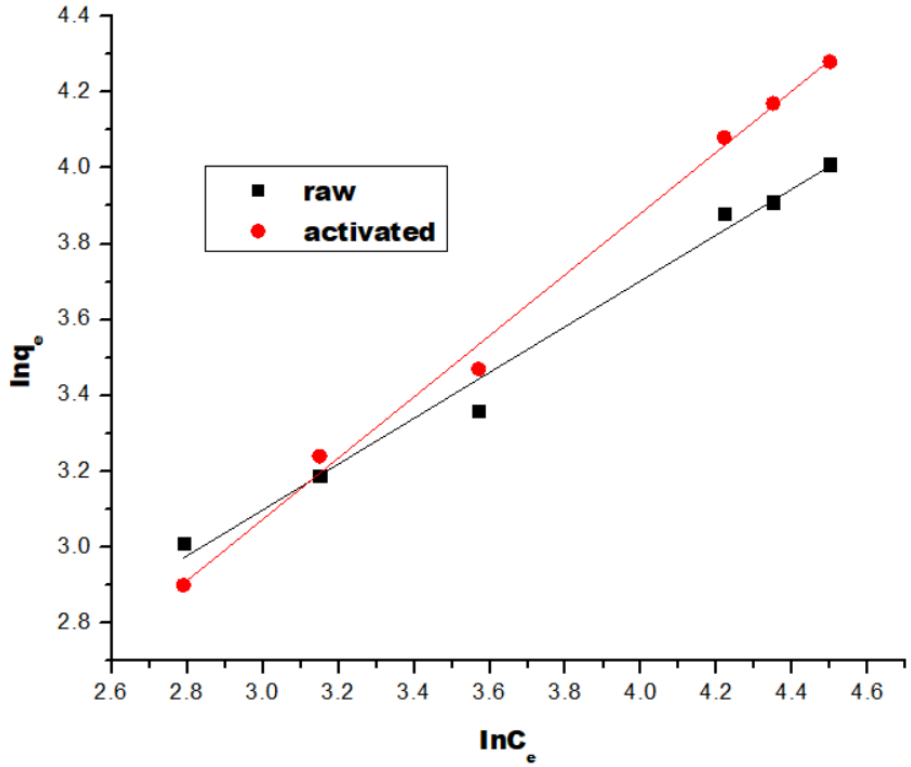

Fig. 9. Freundlich plots for the adsorption of Ni(II) ions by raw and acid-treated sawmill wood waste products

Table 4. Adsorbent Capacity of Sawmill Wood Waste in Comparison with Literature Studies

Adsorbents	Adsorption Capacity (mg/g)	References
Chrysanthemum indicum flowers biochar	44.0	Vilvanathan and Shanthakumar (2016)
Corn cobs hydrochar - alkali-polyethyleneimine modification	29.0	Shi *et al*. (2018)
Corn cobs hydrochar - acid-polyethyleneimine modification	24.5	Shi *et al*. (2018)
Unmodified hydrochar	20.3	Shi *et al*. (2018)
Local rice bran	116.4	Zafar *et al.* (2015)
Fish scale derived nano-rod hydroxyapatite (FSDNHA-800)	114	Edwin *et al*. (2021)
Sugarcane bagasse	123	Blessing *et al*. 2021
Sodium alginate beads / Zeolite Scony Mobile-5	19.6	Mohamed *et al.* (2023)
Copper oxide nanoparticles	15.4	Jain *et al*. (2021)
Pinus sylvestris sawdust	15.7	Chanda *et al*. (2021)
Acid-activated sawmill wood waste products	86.3	Present Study
Raw sawmill wood waste products	78.8	Present Study

Effects of Temperature on Percentage Removal and Thermodynamic Study

The effect of temperature on the adsorption of Ni(II) ions by USWWP and ASWWP revealed distinct trends that indicate temperature-dependent adsorption behavior, as shown in Fig. 10. For the USWWP adsorbent, within a temperature range of 25 to 45 °C, the percentage removal of Ni(II) ions rose from 52.5% at 25 °C to 75.4% at 45 °C, while that of the ASWWP sample increased from 55.4% to a peak of 86.4% at 40 °C, showing a sharper increase in adsorption efficiency compared to the USWWP sample. This increase indicates that raising the temperature up to either 40 or 45 °C enhanced the adsorption efficiency of sawmill wood waste, allowing them to access adsorption sites more readily (Edwin *et al*. 2021). At a much higher temperature of 55 °C, the percentage removal decreased to 65.4% and 72.2% for raw and activated adsorbents respectively, which suggests that higher temperatures may lead to a decline in adsorption capacity. Despite this decline, the ASWWP maintained a higher percentage removal than the USWWP material, indicating that acid activation still provided a more robust adsorption process at elevated temperatures.

The standard thermodynamic equations used to calculate these parameters are shown in Eqs. 11 to 14 (Adeogun *et al*. 2012; Hlihor *et al*. 2015; Ofudje *et al.* 2020),

$$K_d = Q/C_e \quad (11)$$

$$\Delta G = -RTIn(K_d) \quad (12)$$

$$InK_d = \frac{\Delta S}{R} - \frac{\Delta H}{RT} \quad (13)$$

$$\Delta G = \Delta H - T\Delta S \quad (14)$$

where R represents the universal gas constant (8.314 J/mol.K), T is absolute temperature in Kelvin (K), and K_d denotes the equilibrium constant of the adsorption process. A comparative analysis of the thermodynamic parameters for both raw and acid-activated samples were conducted using the data presented in the Fig. 11 with the corresponding values detailed in Table 5.

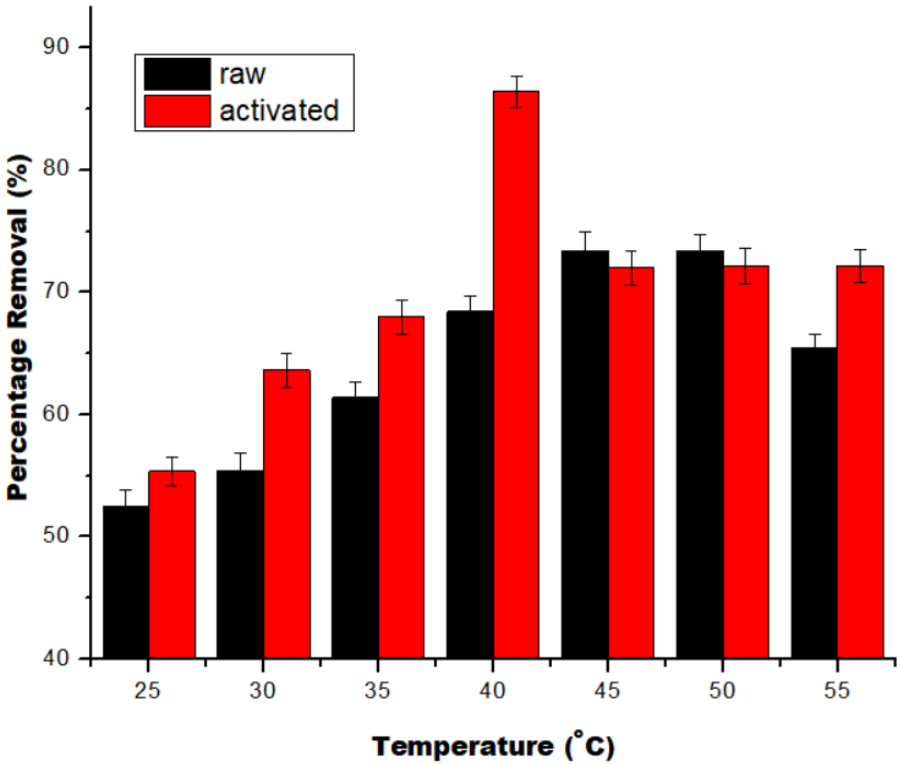

Fig. 10. Percentage removal of Ni(II) ions temperature by raw and acid-treated sawmill wood waste products

For the raw sawmill wood waste, the free energy change (ΔG) ranged from −1.24 to −8.65 kJ/mol, while that of the activated sample ranged from −0.85 to −6.74 kJ/mol across the temperatures tested, showing that adsorption was spontaneous at all temperatures (Ofudje *et al*. 2023). The relatively large range of ΔG values suggests a stronger temperature dependence for the raw material. As temperature increases, the adsorption becomes more spontaneous (more negative ΔG), indicating that temperature positively influenced adsorption on raw wood waste. Though, both raw and acid-treated samples exhibit spontaneous adsorption of Ni(II) ions across all temperatures, but the raw sample showed a broader and more negative range of ΔG compared to the acid-treated sample.

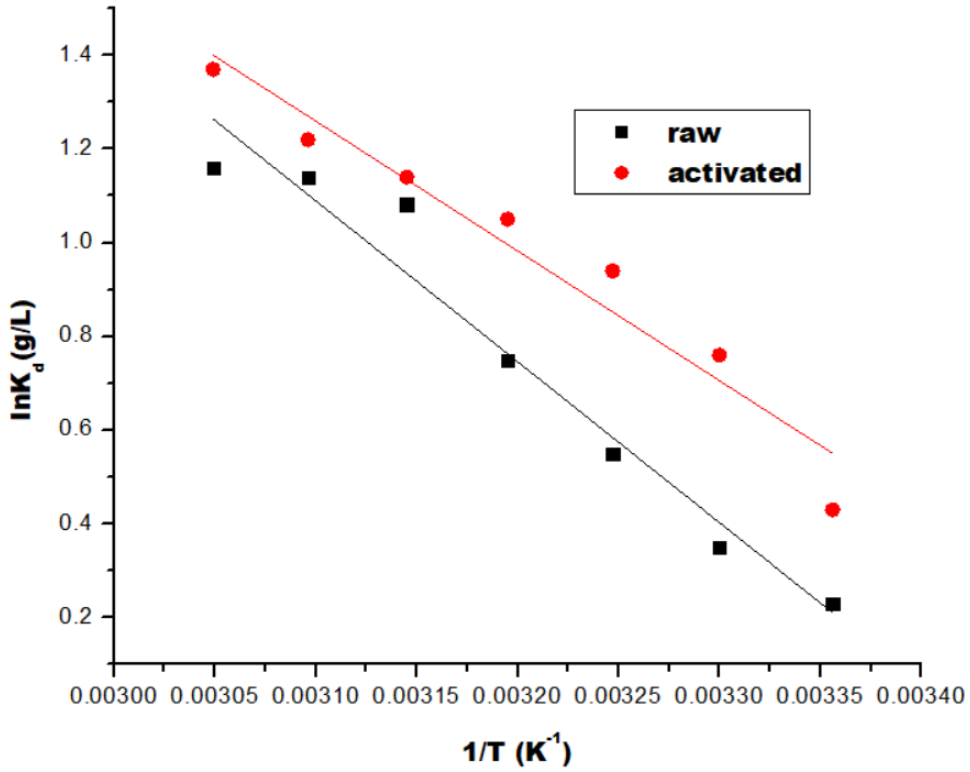

Fig. 11. Thermodynamics plots of Ni(II) adsorption by raw and acid-treated sawmill wood waste products

The value of enthalpy change (ΔH) for raw and activated samples were 10.2 and 23.4 kJ/mol respectively. This positive value indicates that the adsorption process for Ni (II) ions on wood waste was endothermic (Hlihor *et al*. 2015; Ofudje *et al*. 2023), meaning that higher temperatures favor adsorption. The ASWWP sample exhibited a significantly higher positive ΔH value, indicating that the adsorption process is endothermic and more strongly temperature-dependent. This higher enthalpy suggests that acid treatment enhances adsorption by introducing stronger interactions or additional active sites.

The analysis of entropy change (ΔS) showed that the raw and activated sawmill wood waste had values of 4.55 and 8.33 J/mol^{-1}K, and this positive value indicates a slight increase in randomness at the interface upon Ni(II) ion adsorption (Hlihor *et al*. 2015; Ofudje *et al*. 2023). This suggests that adsorbed ions may displace other molecules (such as water) from the surface, leading to a slight increase in disorder. The acid-treated sample showed a higher entropy change, indicating a greater increase in randomness probably due to higher heat supply. This could suggest that acid treatment alters the adsorbent surface, possibly enhancing the release of water molecules or other loosely bound species from the adsorbent surface upon Ni adsorption, resulting in a more disordered state.

Table 5. Key Parameters of Thermodynamic in the Adsorption of Ni(II) by USWWP and ASWWP

Parameter	USWWP	ASWWP
Free Energy Change (kJ/mol)	−1.24 to −8.65	−0.85 to −6.74
Enthalpy Change (kJ/mol)	10.22	23.44
Entropy Change (J/mol·K)	4.55	8.33

Biosorbent Characterization

The Fourier transform infra-red (FT-IR) spectral analysis of sawmill wood waste before and after adsorptions of Ni provides insights into the functional groups involved in the adsorption process. The FT-IR spectrum before adsorption (Fig. 12a) showed long peak intensity at 3488 cm^{-1} corresponding to O-H stretching, which could be attributed to hydroxyl groups from cellulose, hemicellulose, or adsorbed water. The significant broad peak intensity observed indicates strong hydrogen bonding. The peak observed at 2946 cm^{-1} can be assigned to the C-H stretching. of aliphatic hydrocarbons, likely from lignin and cellulose. The C=O stretching observed at 1685 cm^{-1} was attributed to carbonyl groups in lignin or ester linkages. The peaks seen at 1466 and 1374 cm^{-1} correspond to $-CH_2$ bending vibrations in aliphatic chains and C-H bending of methyl groups in lignin or cellulose. The C-O stretching corresponding to alcohols, phenols, or ethers or polysaccharides or lignin were observed at 1225, 1158, and 1019 cm^{-1}, respectively. The C-H out-of-plane bending of aromatic rings in lignin were detected at 967 and 884 cm^{-1}. The FT-IR spectrum after adsorption of Ni ions (Fig. 12b) revealed a peak at 3463 cm^{-1} with reduced intensity, indicating interaction of hydroxyl groups with Ni, possibly through hydrogen bonding or coordination.

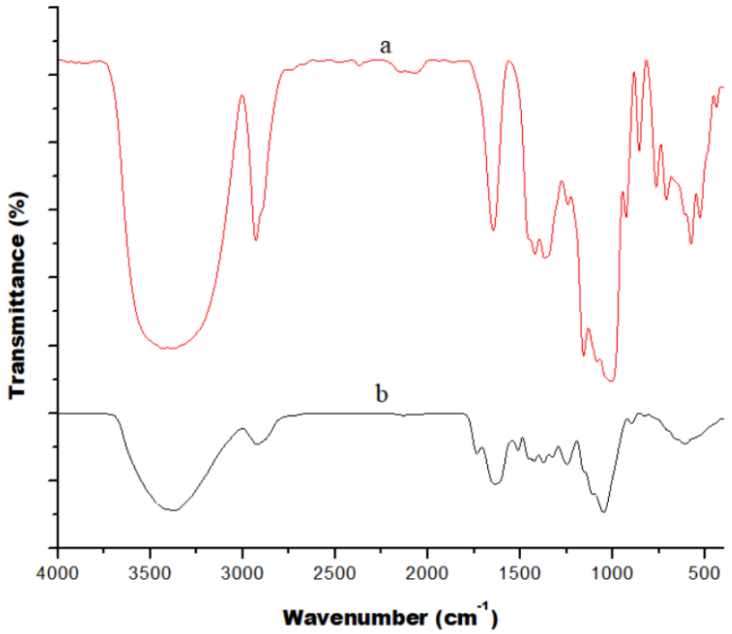

Fig. 12. FT-IR spectra of sawmill wood waste products (a) before and (b) after adsorptions of Ni ions

The observed peak at 2942 cm^{-1} corresponds to C-H bonds, while the one at 1674 cm^{-1} is due to interaction of carbonyl groups with Ni ions, forming coordination bonds. The formation of a new peak at 1561 cm^{-1}, which was absent before adsorption, could suggest the formation of Ni-carboxylate complexes, indicating chemical interaction. Similarly, reduced peak intensities were seen at 1221 and 1149 cm^{-1}, indicating alteration in the C-O stretching vibrations, which is likely due to Ni ions binding to alcohol, phenol, or ether groups, while the one observed at 1014 cm^{-1} indicates changes in polysaccharides or lignin structure due to Ni interaction. In general, the significant shifts in key functional groups (O-H, C=O, and C-O), could suggest their involvement in Ni adsorption, while the appearance of peaks at 1561 and 563 cm^{-1} after adsorption may points to the formation of new complexes, such as Ni-carboxylates and Ni-metal oxides. Reduction in peak intensities could reflect the consumption of active sites on the adsorbent surface during Ni binding. The analysis confirms that hydroxyl, carbonyl, and ether groups may likely be the primary contributors to Ni adsorption, involving mechanisms such as coordination bonding and electrostatic interactions.

Scanning Electron Microscopy (SEM) provides valuable insights into the surface morphology of sawmill wood waste before and after adsorption of Ni ions, as shown in Fig. 13. Before the adsorption of Ni ions, the surface morphology *via* the SEM images typically shows a rough, irregular surface structure with porous networks. These pores are distributed unevenly, indicating the natural fibrous texture of the wood waste. The surface is free from significant particle deposition, displaying clean and well-defined voids. After the adsorption of Ni ions molecules, the surface morphology changed drastically, revealing significant changes in surface texture. The pores and voids initially observed were completely blocked. The surface appears smoother compared to the pre-adsorption state, attributed to Ni ion coverage.

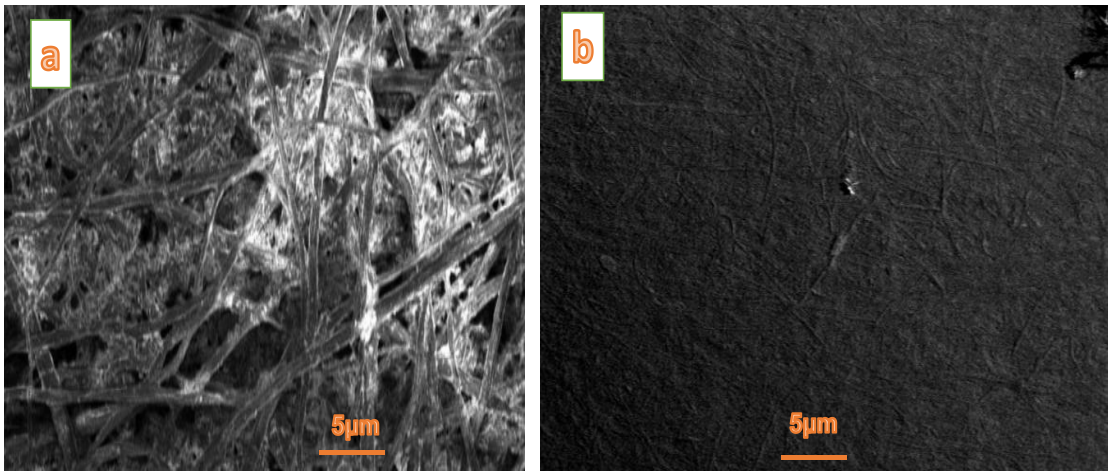

Fig. 13. SEM of sawmill wood waste **(a)** before, and **(b)** after adsorption of Ni(II) ions

CONCLUSIONS

The use of sawmill wood waste products for the sorption of Ni(II) ions *via* batch process from aqueous solution under the influence of variables like initial Ni concentration, contact time, dosage, pH, and temperature was examined. Raw and acid-activated sawmill wood wastes were used, and the results obtained are summarized below:

1. Both unactivated sawmill waste product (USWWP) and acid-activated sawmill waste product (ASWWP) reached maximum adsorption efficiency at a pH of 5.

2. ASWWP sample had a higher maximum adsorption (Q_{max}) value of 86.3 mg/g than the raw sample (78.8 mg/g), indicating that acid activation enhances the maximum adsorption capacity by increasing surface area and available adsorption sites.

3. The pseudo-first-order kinetic model fit well for the raw sawmill wood waste, as shown by high R^2, low %SSE, and close alignment between $q_{e\{exp\}}$ and $q_{e\{cal\}}$. By contrast, the pseudo-second-order kinetic model was found to be especially well-suited for describing the adsorption of Ni(II) ions on acid-treated sawmill wood waste.

4. With a higher K_f, lower $1/n$, and better R^2, the Freundlich isotherm model was more effective in the case of ASWWP adsorbent, whereas USWWP sample is well predicted by Langmuir isotherm.

ACKNOWLEDGMENTS

The authors extend their appreciation to the financial support *via* the Researchers Supporting Project number (RSPD2025R754) from King Saud University, Riyadh, Saudi Arabia for funding this research.

REFERENCES CITED

Adeogun, A. I., Ofudje, E. A., Idowu, M. A., and Ahmed, S. A. (2012). "Biosorption of Cr(VI) ion from aqueous solution by maize husk: Isothermal, kinetic and thermodynamic study," *J. Chem. Soc. Pak.* 34, 1388-1396.

Adeogun, A. I., Ofudje, E. A, Idowu, M. A., Kareem, S. O., Vahidhabanu, S., and Ramesh, B. (2018). "Biowaste derived hydroxyapatitefor the effective removal of reactive yellow 4 dye: Equilibrium, kinetic and thermodynamic studies," *Ame. Chem. Soc. Omega* 3, 1991-2000. DOI: 10.1021/acsomega.7b01768.

Akpomie, K. G., and Dawodu, F. A. (2014). "Treatment of an automobile effluent from heavy metals contamination by an eco-friendly montmorillonite," *J. Adv. Res.* 6, 1003-1013. DOI: 10.1016/j.jare.2014.12.004

Blessing, A. E., Dauda, A. M., Clement, M. Z. W., Wisdom, S. J., Athanasios, A., Sara, T. E., Naeem, Q., Clement, A. Y., and Gaber, El-S. B. (2021). "Agricultural waste of sugarcane bagasse as efficient adsorbent for lead and nickel removal from untreated wastewater: Biosorption, equilibrium isotherms, kinetics and desorption studies," *Biotechnology Reports* 30, e00614. DOI: 10.1016/j.btre.2021.e00614

Buxton, S., Garman, E., Heim, K. E., Lyons-Darden, T., Schlekat, C. E., Taylor, M. D., and Oller, A. R. (2019). "Concise review of nickel human health toxicology and ecotoxicology," *Inorganics* 7(7), 89. DOI: 10.3390/inorganics7070089

Chanda, R., Mithun, A. H., Hasan, M. A., and Biswas, B. K. (2021). "Nickel removal from aqueous solution using chemically treated mahogany sawdust as biosorbent," *J. Chem.* 1-10. DOI: 10.1155/2021/4558271

Chukwuemeka-Okorie, H. O., Ekemezie, P. N., Akpomie, K. G., and Olikagu, C. S. (2018). "Calcined corncob-kaolinite combo as new sorbent for sequestration of toxic metal ions from polluted aqua media and desorption," *Front. Chem.* 6, 1-13. DOI: 10.3389/fchem.2018.00273.

Edwin, A. O., Adebusayo, E. A., Olugbenga, B. O., Ezekie, F. S., Francis, H. I., and Dan, Z. (2021). "Nano-rod hydroxyapatite for the uptake of nickel ions: Effect of sintering behaviour on adsorption parameters," *J. Environ. Chem. Eng.* 9, article 105931. DOI: 10.1016/j.jece.2021.105931

Dragana, B., Gorgievski, M., Stanković, V., Štrbac, N., Šerbula, S., and Petrović, N. (2013). "Adsorption of heavy metal ions by beech sawdust – Kinetics, mechanism and equilibrium of the process," *Ecolo. Eng.* 58, 202-206. DOI: 10.1016/j.ecoleng.2013.06.03

Duran, C., Ozdes, D., Gundogdu, A., and Senturk, H. B. (2011). "Kinetics and isotherm analysis of basic dyes adsorption onto almond shell (*Prunus dulcis*) as a low cost adsorbent," *Journal of Chemical & Engineering Data* 56(5), 2136-2147. DOI: 10.1021/je101204j

Jain, M., Yadav, M., and Chaudhry, S. (2021). "Copper oxide nanoparticles for the removal of divalent nickel ions from aqueous solution," *Toxin Review* 40, 872-885. DOI: 10.1080/15569543.2020.1799407

Hlihor, R. M., Diaconu, M., Leon, F., Curteanu, S., Tavares, T., and Gavrilescu, M. (2015). "Experimental analysis and mathematical prediction of Cd (II) removal by biosorption using support vector machines and genetic algorithms," *New Biotechnol*. 32, 358-368. DOI: 10.1016/j. nbt.2014.08.003

Hubbe, M. A., Azizian, S., and Douven, S. (2019). "Implications of apparent pseudo-second-order adsorption kinetics onto cellulosic materials. A review," *BioResources* 14(3), 7582-7626. DOI: 10.15376/biores.14.3.7582-7626

Izinyon, O. C., Nwosu, O. E., Akhigbe, L. O., and Ilaboya, I. R. (2016). "Performance evaluation of Fe (III) adsorption onto brewers' spent grain," *Niger. J. Technol.* 35, 970-978. DOI: 10.4314/njt.v35i4.36

Kovacova, Z., Demcak, S., Balintova, M., Pla, C., and Zinicovscaia, I. (2020). "Influence of wooden sawdust treatments on Cu(II) and Zn(II) removal from water," *Materials*, 13, article 3575. DOI:10.3390/ma13163575

Li, X., Wang, Y., Cui, X., Lou, Z., Shan, W., Xiong, Y., and Fan, Y. (2018). "Recovery of silver from nickel electrolyte using corn stalk-based sulfur-bearing adsorbent," *Hydrometallurgy* 176, 192-200. DOI.10.1016/j.hydromet.2018.01.024

Liu, X., Xu, X., Dong, X., and Park, J. (2020). "Competitive adsorption of heavy metal ions from aqueous solutions onto activated carbon and agricultural waste materials," *Pol. J. Environ. Stud*. 29, 749-761. DOI: 10.15244/pjoes/104455

Mahdi, Z., Yu, Q. J., and El- Hanandeh, A. (2018). "Investigation of the kinetics and mechanisms of nickel and copper ions adsorption from aqueous solutions by date seed derived biochar," *J. Environ. Chem. Eng.* 6, 1171-1181. DOI: 10.1016/j.jece.2018.01.021

Mohamed, S. H., Ahmed, M. R., Kishore, K. K., Sayed, K. A., and Mariam, E. F. (2023). "Adsorption characteristics of nickel (II) from aqueous solutions by Zeolite Scony Mobile-5 (ZSM-5) incorporated in sodium alginate beads," *Sc. Rep.* 13, article 19601. DOI: 10.1038/s41598-023-45901-x

Nirav, P. R., Prapti, U. S., and Nisha, K. S. (2016). "Adsorptive removal of nickel(II) ions from aqueous environment: A review," *J. Environ. Mgt.* 179, 1-20. DOI: 10.1016/j.jenvman.2016.04.045

Ofudje, E. A., Awotula, A. O., Alayande, S.O., Asogwa, K. K., and Olukanni, O. D. (2014). "Removal of lead (II) ions from aqueous solution by *Tricholoma terreum:* Kinetic studies," *Adv. in Res.* 2(2), 58-69.

Ofudje, E. A., Awotula, A. O., Hambate, G. V., Akinwunmi, F., Alayande, S. O., and Olukanni, O. D. (2017). "Acid activation of groundnut husk for copper adsorption: Kinetics and equilibrium studies," *Desalin. and Water Treat.* 86, 240-251. DOI: 10.5004/dwt.2017.21339.

Ofudje, E. A., Adeogun, A. I., Idowu, M. A., Kareem, S. O., and Ndukwe, N. A. (2020). "Simultaneous removals of cadmium (II) ions and reactive yellow 4 dye from aqueous solution by bone meal derived apatite: Kinetics, equilibrium and thermodynamic evaluations," *J. Anal. Sci. and Tech.* 11, article 7. DOI: 10.1186/s40543-020-0206-0

Ofudje, E. A., Sodiya, E. F., Olanrele, O. S., and Akinwunmi F. (2023). "Adsorption of Cd^{2+} onto apatite surface: Equilibrium, kinetics and thermodynamic studies," *Heliyon*. DOI: 10.1016/j.heliyon.2023.e12971

Sahoo, P., and Das, S. K. (2011). "Tribology of electroless nickel coatings—A review," *Mater. Des.* 32, 1760-1775. DOI: 10.1016/j. matdes.2010.11.013

Shi, Y., Zhang, T., Ren, H., Kruse, A., and Cui, R. (2018). "Polyethylene imine modified hydrochar adsorption for chromium(VI) and nickel(II) removal from aqueous solution," *Bioresource Technol.* 247, 370-379. DOI: 10.1016/j.biortech.2017.09.107

Shrestha, R., Ban, S., Devkota, S., Sharma, S., Joshi, R., Tiwari, A. P., Hark, Y.K., and Joshi, M. K. (2021). "Technological trends in heavy metals removal from industrial wastewater: A review," *J. Environ. Chem. Eng.* 9, article 105688. DOI: 10.1016/j.jece.2021.105688

Sudha, R., Srinivasan, K., and Premkumar, P. (2015). "Removal of nickel(II) from aqueous solution using c*itrus limettioides* peel and seed carbon," *Ecotox. and Environ. Safety* 117, 115-123. DOI: 10.1016/j.ecoenv.2015.03.025

Vilvanathan, S., and Shanthakumar, S. (2016). "Ni(II) adsorption onto *Chrysanthemum indicum*: Influencing factors, isotherms, kinetics, and thermodynamics," *Int. J. Phytorem.* 18, 1046-1059. DOI: 10.1080/15226514.2016.1183575

Wasefa, B., Summi, R., Soujanya, B., Sudip, B., Monohar, H. M., Ajaya, B., and Bidyut, S. (2022). "A comprehensive review on the sources, essentiality and toxicological profile of nickel," *RSC Adv.* 12(15), 9139-9153. DOI: 10.1039/d2ra00378c

Yanovska, E., Savchenko, I., Petrenko, O., and Davydov, V. (2022). "Adsorption of some toxic metal ions on pine sawdust in situ immobilized by polyaniline," *Appl. Nanosci.* 12, 861-868. DOI: 10.1007/s13204-021-01862-z

Zafar, M. N., Aslam, I., Nadeem, R., Munir, S., Rana, U. A., and Khan, S. U. D. (2015). "Characterization of chemically modified biosorbents from rice bran for biosorption of Ni(II)," *J. Taiwan Inst. Chem. Eng.* 46, 82-88.

Article submitted: December 18, 2024; Peer review completed: February 1, 2025;
Revisions accepted: February 7, 2025; Published: March 4, 2025.
DOI: 10.15376/biores.20.2.3024-3046